ICAS-98-3,10,5

A98-31571

BOUNDARY LAYER EFFECTS ON THE BASE PRESSURE BEHIND A BLUNT TRAILING EDGE AEROFOIL

Kaliope Vassilopoulos and Sudhir L. Gai

School of Aerospace and Mechanical Engineering
University College
University of New South Wales
The Australian Defence Force Academy
CANBERRA, AUSTRALIA

Abstract

The nature of the boundary layer at the point of separation from a plain blunt trailing edge aerofoil was examined to determine its effect on the base pressure in the near wake. Tests were conducted in a low turbulence subsonic wind tunnel, with and without end plates. The results show that with a laminar boundary layer and end plates, the region of nominally two dimensional vortex shedding was more than doubled. The turbulent boundary layer reduces the mean base pressure coefficient, but unlike the laminar boundary layer, does not extend the region of nominally two dimensional flow. The fluctuating pressure signals suggest that the turbulent boundary layer also improves the two dimensionality of the shedding vortex street as evidenced by the significantly larger, well correlated, pressure fluctuations.

Introduction

There have been numerous studies over the years into the near wake structure of circular cylinders, with particular emphasis on steady state aspects of the flow and the effect of end plates on vortex shedding. Only recently has serious thought been given to the near wake structure of blunt trailing edge geometries, such as Tombazis and Bearman[1],Bearman[2], Bearman and Tombazis[3], Petrusma and Gai [4,5], and Vassilopoulos *et al*[6]. Unlike cylinder flows where major effort has been expended, little is known about the unsteady flow characteristics behind such blunt trailing edge geometries.

Previous work has also shown that by direct manipulation of the end constraints, different shedding modes along the span could be induced, for example Gerich and Eckelmann [7], Szepessy and Bearman[8], Shair *et al* [9], and Hammache & Gharib[10]. Investigations into different shedding modes in cylinder wakes, though, have been mainly confined to high model aspect ratios, usually more than 100 [11], with little data available for low to moderate aspect ratios (AR < 40)[12]. As such, a full appreciation of the effect of end constraints on vortex shedding is still lacking in the literature.

Many of these aforementioned studies have primarily examined the effect of a turbulent separating boundary layer on the near wake flow in order to avoid the complications of natural transition. Thus the influence of the state of the boundary layer at the model trailing edge on the unsteady wake has received little attention.

As has been reported in many investigations, such as Maull & Young [13], Bearman[14,15], Williamson & Roshko [16], and Petrusma and Gai [4], the base pressure does not remain constant across the model span except for a small region around the mid span where the flow could be said to be nominally two dimensional. This phenomenon was shown to be strongly influenced by end constraints, as shown by Bearman[14] who determined that use of end plates reduced the base pressure coefficient by 2-3%.

The present study was therefore undertaken to investigate the unsteady characteristics of the flow in the near wake region of a blunt trailing edge aerofoil subject to various end constraints and particularly the effect of the separating boundary layer state. This would be achieved through the analysis of fluctuating base pressures along the model span, the spanwise mean base pressure coefficient, the correlation coefficient and the Fourier analysis of the spanwise fluctuating pressures.

Experimental Arrangement & Techniques

The experiments were conducted in an open circuit subsonic wind tunnel of 457 mm x 457 mm test section with a free stream turbulence level of 0.2%. A modified NACA 0012 aerofoil with a plain blunt trailing edge, spanning the wind tunnel, was used for all tests.

End plates as specified by Stansby[17] were also used, reducing the model aspect ratio (span/base height) from 30 without end plates to 20 with end plates, as shown in figure 1. The Reynold's number based on a free stream velocity of 20 m/s and model chord was 1.6×10^5.

Without a roughness strip, hot wire measurements established that the separating boundary layer just upstream of the trailing edge was laminar. Using a roughness strip, positioned between 15% and 22% of the

model chord from the leading edge, the separating boundary layer was found to be turbulent.

Fluctuating base pressures were recorded using ENDEVCO 8507C-2 miniature pressure transducers with a pressure range of 0 - 2 psi, fitted into the base, and vented to the atmosphere. Each transducer was fitted in a brass plug for ease in movement along the model span. All transducers were calibrated in situ before use. Their output was fed into a PC30 A-D board and analysed using a program written for this purpose.

Three pressure transducers were used with transducer #1 fixed at the centre, and transducers #2 and #3 located on either side along the spanwise axis. Due to manufacturing constraints, at position 18 which is the model centre, the transducers are located two base heights apart. Similarly, due to the placement of the end plates, the furthest position available for measurements was position 4, nine base heights either side from the centre.

The fluctuating base pressures were recorded at a sampling rate of 10 kHz, and then transducers #2 and #3 were moved at half base height intervals progressively outwards. This process was repeated for all positions, with and without end plates, for laminar and turbulent boundary layer conditions.

The pressure signals were also connected to an ONI SOKKI Frequency Analyser which gave the Fourier Transform of the fluctuating base pressure signals directly. This process was undertaken for all positions along the span, with and without end plates, for laminar and turbulent boundary layer conditions.

Results and Discussion

Fluctuating Base Pressures:

The fluctuating pressures were normalised with respect to the r.m.s. pressure and plotted against time normalised with respect to the Strouhal period for this analysis.

At position 18, with a laminar boundary layer and without end plates, the normalised pressure traces exhibited similar signatures and magnitude of fluctuations. When end plates were used, the signatures for all three transducers were stronger and the magnitude of the fluctuations increased. For this test condition, end plates therefore promoted flow symmetry.

When the separating boundary layer was turbulent, the normalised pressure traces at position 18 showed a significant increase in the magnitude of fluctuations, almost double that of the laminar results, regardless of end constraints. At this position, the signature of all normalised pressures remained pronounced. From these results, it was concluded that although a turbulent boundary layer enhanced the separating vortex street, use of end plates seemed to have little effect on the shedding vortex street.

As the transducers were moved outwards away from the centre, the fluctuating pressure signals remained relatively constant for a short region mid span before showing any changes in either phase or magnitude. When the separating boundary layer was laminar, this region of nominally two dimensional flow extended to six base heights without end plates, and to ten base height with end plates. When the separating boundary layer was turbulent, the region of nominally two dimensional flow extended to fourteen base heights without end plates, more than double that of the laminar boundary layer, and to ten base height with end plates, which remained unchanged.

The ratio of the effective two dimensional mid span region to the geometric aspect ratio of the model could be used as a means of comparing the changing flow characteristics directly. For example, the model aspect ratio without end plates for a laminar boundary layer is 30, and the two dimensional region for this same condition was seen to extend for 6 base heights across the model centre. The ratio of the two dimensional region to the aspect ratio is therefore 0.2. With end plates, this ratio increased to 0.5, a significant improvement in the two dimensionality of the vortex shedding. When the boundary layer was turbulent, this ratio becomes 0.5, regardless of end constraints. This comparison shows that although a significant improvement could be achieved with end plates and a laminar boundary layer, end plates have little effect with a turbulent separating boundary layer.

At the furthest position, when transducers #2 and #3 were nine base heights from the centre, the traces for a laminar separating boundary layer revealed that regardless of the end constraints, the pressure signals of transducers #2 and #3 were attenuated. Here, the normalised pressures exhibit a considerable phase drift with a significant reduction in signal magnitude as well as signature compared to that of the central transducer #1. This would also indicate that vortex shedding is no longer two dimensional at this position. At this extreme position, one would expect maximum end wall effects which were clearly seen by the signal attenuation and asymmetry of transducers #2 and #3.

At this same position with a turbulent separating boundary layer, the results showed that regardless of the end constraints, the signature for all transducers remained relatively strong, with large magnitude of fluctuations still evident. When end plates were used, small regions of signal attenuation were seen to occur, but for the most part, a discernible signature remained. Without end plates, these small attenuation regions were eliminated. This phenomenon would again be caused by wall interference, which is expected to occur at this extreme position, but as the boundary layer is now turbulent, the effect is smaller.

From the above analysis of the fluctuating pressure signals, it can be seen that a turbulent boundary layer has a greater effect on the two dimensionality of the flow, promoting strong vortex shedding along the entire model span. A laminar boundary layer, though, seems more susceptible to end effects as evidenced by the significant signal attenuation with increasing spanwise distance away from the model centre. The positive influence of end plates on the flow was shown to improve the two dimensionality of the flow with a laminar boundary layer, but diminished when the separating boundary layer was turbulent.

The turbulent boundary layer results showed a prominence of intermittent bursts of high frequency fluctuations regardless of the end constraints. This would

suggest that the vortex shedding is more likely to be parallel, while with a laminar boundary layer it is more likely to be oblique. Such a scenario is possible because with a turbulent boundary layer, shear layer instability waves, which give rise to these intermittent bursts of high frequency fluctuations, would be more predominant with parallel shedding[18], and consequently more nearly two dimensional flow. Hence the effects of end plates will be less significant with a turbulent boundary layer.

Mean Base Pressure Coefficient:

The spanwise mean base pressure coefficient, as defined below, was calculated both with and without end plates and with a laminar and turbulent separating boundary layer.

$$\overline{C_p} = \frac{\overline{p} - p_\infty}{\frac{1}{2}\rho U_\infty^2} \qquad (1)$$

Here, $\overline{p}$ is the mean base pressure, p_∞ is the free stream static pressure, and $\frac{1}{2}\rho U_\infty^2$ is the free stream dynamic pressure.

The spanwise distribution of the base pressure coefficient for a laminar separating boundary layer is presented in figure 2, while that for a turbulent boundary layer is shown in figure 3. When the separating boundary layer was laminar, a distinct reduction in the base pressure coefficient with increasing spanwise distance from the centre is evident, regardless of end constraints. With end plates, the base pressure coefficient at the model centre was -0.53 compared to -0.55 without end plates. The lower value without end plates is possibly the result of the laminar base flow interacting with a thick turbulent tunnel wall boundary layer. These results seem to be consistent with the work of Williamson and Roshko [16], who found that for low model aspect ratios, less that about 30, a reduction in aspect ratio would increase the base pressure coefficient.

When the separating boundary layer was turbulent, the results once again show a decreasing base pressure coefficient with increasing spanwise distance as seen in figure 3. The value of the mean base pressure coefficient is -0.52 with no end plates, and -0.587 with end plates. The lower base pressure coefficient with end plates is due to the fact that the turbulent base flow is not heavily influenced by the comparatively thin boundary layers of the end plates themselves. The value of -0.587 for the base pressure coefficient with end plates corresponds well with Bearman and Tombazis[3] and Tombazis [19] for similar test conditions.

Unlike the laminar case, the turbulent boundary results contradict Williamson and Roshko[16], in the sense that as aspect ratio is reduced, base pressure decreases. These results though support the findings of Bearman[14] who determined that end plates may reduce the base pressure coefficient by 2-3%. This phenomenon may not be experienced when the boundary layer is laminar because along the entire span, end effects dominate.

According to Williamson and Roshko[16], oblique shedding always gives higher base pressures with a laminar boundary layer. A laminar boundary layer combined with a low aspect ratio would therefore yield a higher base pressure, as evident in the above results. With a turbulent boundary layer, the above results suggest that the shedding is more likely to be parallel, which in turn results in a lower base pressure. As the aspect ratio is reduced further through the use of end plates, the base pressure will decrease because of enhanced parallel shedding.

Correlation of Fluctuating Base Pressures:

The correlation between two pressure signals along the span, as referenced to transducer #1, was calculated as:

$$R_{p_{ij}} = \frac{\overline{\left(P_i' - P_{i_{rms}}\right)\left(P_j' - P_{j_{rms}}\right)}}{\sqrt{\overline{\left(P_i' - P_{i_{rms}}\right)^2}\,\overline{\left(P_j' - P_{j_{rms}}\right)^2}}} \qquad (2)$$

The results for a laminar boundary layer are presented in figure 4, while those for a turbulent boundary layer are presented in figure 5. From these figures, regardless of end constraints or state of the boundary layer, the correlation coefficient decreases with increasing distance away from the model centre.

A line of best fit through each set of test results, as shown in the figure, indicates that the rate of decay of base pressure correlation coefficient with increasing spanwise distance is more pronounced without end plates than with end plates. This increased decay rate without end plates is evident regardless of the state of the separating boundary layer, and would suggest that three dimensional effects are more evident when the span extends across the tunnel walls.

Near the model centre, a higher correlation coefficient is evident with end plates than without, suggesting a stronger orderly vortex shedding in this region. The above results are in agreement with Bearman[2] whose findings are also presented here for comparison. The initial rapid decline in the correlation coefficient could be due to three dimensional velocity fluctuations resulting from spanwise phase variations in vortex shedding.

Therefore, as the mean flow has been shown to suffer from three dimensional effects, the correlation between instantaneous fluctuating pressures would not also be high[20].

The reason why the magnitude of the correlation coefficient for a turbulent boundary layer is smaller than that of a laminar boundary layer is that with a turbulent boundary layer, the wake is more likely to consist of non-homogeneous vortex shedding in which individual cells are independent of each other.

Another possible explanation for this is that due to the high frequency bursts, as observed in the fluctuating pressure traces, the actual correlation length is reduced significantly, reducing the correlation coefficient. The small correlation coefficient values could also imply that the turbulent flow patterns are highly independent and that in fact, vortex shedding is occurring in cells with different characteristic frequencies along the span. Previous work conducted by the authors[22] showed that in fact several distinct shedding frequencies were recorded along the model span, and the number and magnitude of

these frequencies depended on the end constraints employed and the state of the boundary layer.

At the high Reynold's number of this test program, the three dimensional effects could have been triggered by the higher levels of turbulence in the flow, which would introduce disturbances to the shear layer. Previous investigations[8,19,21] have already established that it is in fact the state of the shear layer rather than the boundary layer before separation that has a major effect on vortex shedding. The shear layer instabilities therefore play a significant part in defining the near wake flow characteristics.

Even when the signals were filtered, the correlation coefficient did not markedly improve. Evaluation of the coherence of the data was not available at the time of writing but it is hoped that this analysis should shed some light on these results.

Frequency Signal Analysis:

The vortex shedding frequency along the span was recorded using the Fourier analysis of the fluctuating pressure signals. The shedding frequency will be presented in terms of the Strouhal number which is defined as:

$$S = \frac{fh}{U_\infty} \qquad (3)$$

Here h is the model base height, U_∞ is the free stream velocity, and f is the shedding frequency.

With a laminar separating boundary layer the spanwise Strouhal number distribution is shown in figure 6 with and without end plates. This figure shows one dominant frequency corresponding to a Strouhal number of 0.232 for all spanwise positions, regardless of end constraints. As the shedding seems to be dominated by this frequency, the other shedding frequencies need to be fairly strong, otherwise they would be masked by the wall effects. When end plates were used, the variation of Strouhal number across the span was more orderly, with only one additional shedding frequency compared to three additional frequencies with no end plates.

With a turbulent boundary layer, the spanwise distribution of Strouhal number is shown in figure 7, with and without end plates. The results show a significant increase in the number of frequencies recorded, regardless of the end conditions. Despite this increase in the number of discrete frequencies, the Strouhal number variation was minimal. Similar to the laminar case, this figure also shows one dominant frequency corresponding to a Strouhal number of 0.232, for all spanwise stations. There is also greater scatter in the three extra frequencies recorded without end plates, and the additional five frequencies recorded with end plates.

Discussion

The detailed spanwise fluctuating base pressures illustrate the complex three dimensional nature of the near wake flow behind the plain blunt trailing edge geometry. Regardless of the type of end constraints employed, the low model aspect ratio ensured that end effects dominated across the entire model span.

The state of the boundary layer was also seen to play a significant role in the spanwise flow behaviour. We find that with end plates and a laminar separating boundary layer, the flow is generally more ordered. End plates suppress the cross flow leading to an enhancement of vortex shedding uniformity. On the other hand, without end plates, there are a number of frequency cells caused by transverse pressure gradients which induce cross flow along the span.

Shear layer instability waves inherent to boundary layers are clearly seen in the pressure-time spectra as high frequency bursts. They are similar to the velocity-time spectra of Prasad and Williamson[18]. These shear layer instabilities are also evident in the spanwise correlation coefficient distribution. The high frequency bursts seem to dominate the flow, resulting in a very short correlation length, and very poor correlation overall.

With a turbulent boundary layer, the shear layer instability waves are stronger and regular and the flow, on average, appears more orderly with very nearly parallel shedding. In other words, the effect of end plates is not significant. Once again, the fact that vortex shedding is more likely to be parallel with higher Reynold's number and turbulent flow than with low Reynold's number and laminar flow, is consistent with earlier observations[18].

An important feature to emerge from these experiments is that with a plain blunt trailing edge, the near wake flow is dominated by vortex shedding occurring with multiple frequencies and multiple cells which are seemingly independent of each other. These findings support the conjectures made by Bearman and Tombazis[3].

Conclusions

Detailed fluctuating pressure measurements along the span of a blunt trailing edge aerofoil have revealed the highly complex nature of the near wake flow. The influence of confining walls cannot be ignored in cases of low to moderate aspect ratio, as the nature of the shedding vortex street has been shown to be dominated by end plates and model aspect ratio.

The influence of the state of the boundary layer at separation on both unsteady and mean base pressures has been shown to be significant. The results have shown that a more two dimensional flow with parallel vortex shedding is likely to be obtained with a turbulent boundary layer. The results also show that a decrease in model aspect ratio promotes more parallel shedding which will decrease the base pressure.

From the data, it would seem that the strong shear layer instability waves with a turbulent separating boundary layer would have a greater influence on vortex shedding, supporting the work of Sieverding and Heinemann[21], and Prasad and Williamson[18].

References

1 Tombazis, N., and Bearman, P.,(1997), *J. of Fluid Mechanics*, Vol 330. pp85-112.

2 Bearman, P.W., (1992), Proc., IUTAM Symposium on Bluff Body Wakes, Dynamics and Instabilities, Gottingen.

3 Bearman, P.W., and Tombazis, N., (1992), 2nd. Int. Colloquium on Bluff Body Aerodynamics, Melb., Aust.

4 Petrusma, M.S., and Gai, S.L., (1994), *Aero. Journal*, Aug.-Sep., pp 267-74.

5 Petrusma, M.S., and Gai, S.L., (1996), *Experiments in Fluids*, Vol. 20, pp 189-198.

6 Vassilopoulos, K., Gai, S.L., and Petrusma, M.S., (1995), *33rd Aerospace Sciences Meeting and Exhibit*, Jan 9-12, Reno, NV, Paper AIAA 95-0531.

7 Gerich, D., and Eckelmann, H., (1982), *J. of Fluid Mechanics*, Vol. 122, pp 109-21.

8 Szepessy, S., and Bearman P.W., (1992), *J. of Fluid Mechanics*, Vol. 234, pp 191-217

9 Shair, F.H., Grove, A.S., Petersen, E.E., and Acrivos, A., (1963), *J. of Fluid Mechanics*, May, pp 546-550.

10 Hammache, M., and Gharib, M., (1991), *J. of Fluid Mechanics*, Vol. 232, pp 567-90.

11 Lee, T., and Budwig, R., (1991), *Physics of Fluids*, Vol. 3, part 2, pp 309-15.

12 Williamson, C.H.K., (1989), *J. of Fluid Mechanics*, Vol. 206, pp 579-627.

13 Maull, , and Young, (1973), *J. of Fluid Mechanics*, Vol. 60 part 2, pp 401-9.

14 Bearman, P.W., (1965), *J. of Fluid Mechanics*, Vol. 21 part 2, pp 241-55.

15 Bearman, P.W., (1967), *Aero. Quart.*, Vol. 18, pp 207-24.

16 Williamson, C.H.K, and Roshko, A., (1990), Z. Flugwiss Weltraunforsch, Vol. 14, Springer-Verlag, pp 38-46.

17 Stansby, P.K., (1974), *Aero. Journal.*, Jan. pp 36-37.

18 Prasad, and Williamson, C.H.K., (1997), *J. of Fluid Mechanics*, Vol. 333, pp375-422.

19 Tombazis, N., (1993) PhD Thesis, Imperial College, UK.

20 Cherry, N.J., Hillier, R., and Latour, M.E.M.P., (1984), *J. of Fluid Mechanics*, Vol. 144, pp 13-46.

21 Sieverding, C.H., and Heinemann, H., (1990), *J .of Turbomachinery*, Vol. 112, pp 181-187.

22 Vassilopoulos, K., and Gai, S.L., (1996), 20th Congress of ICAS, Sorrento, Italy.

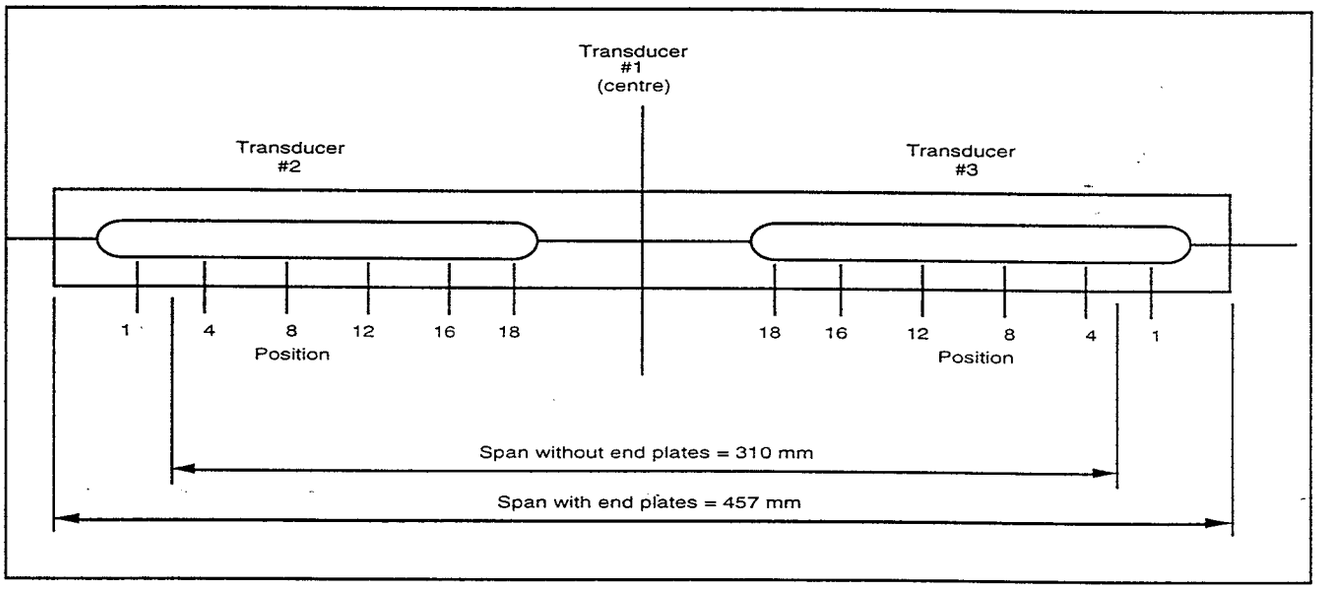

FIGURE 1: Rear view of model.

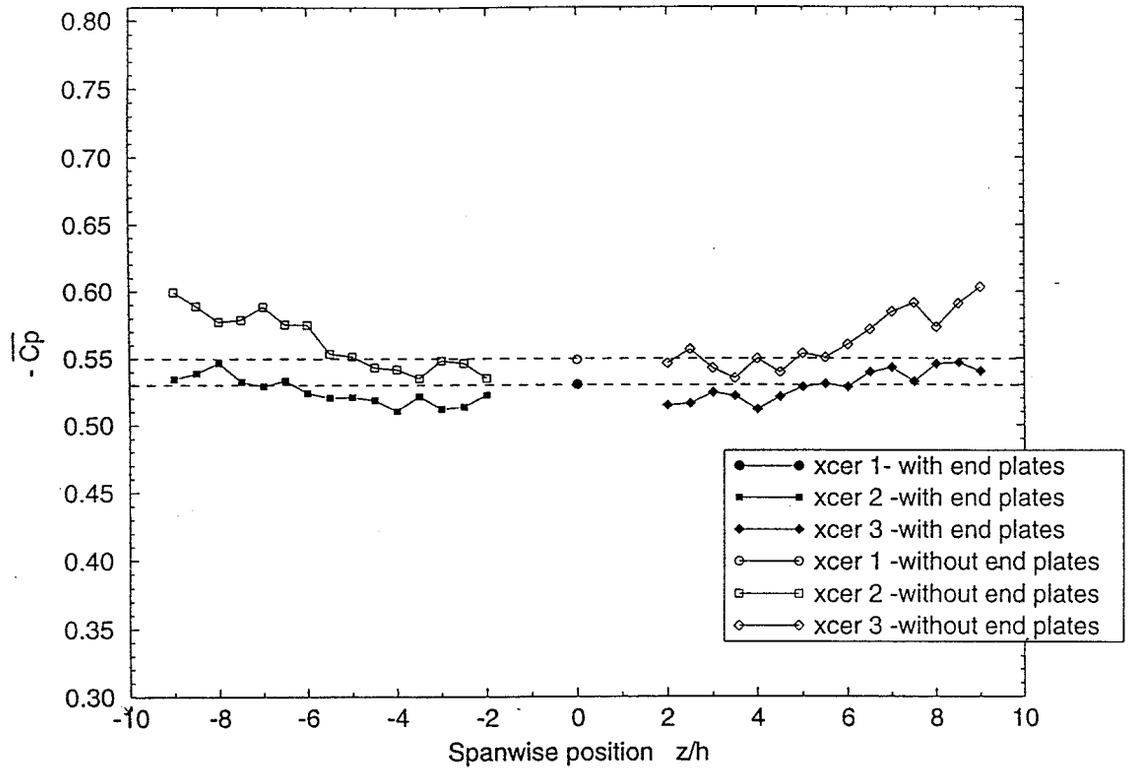

FIGURE 2: Mean Base Pressure Coefficient
-Laminar Boundary Layer-

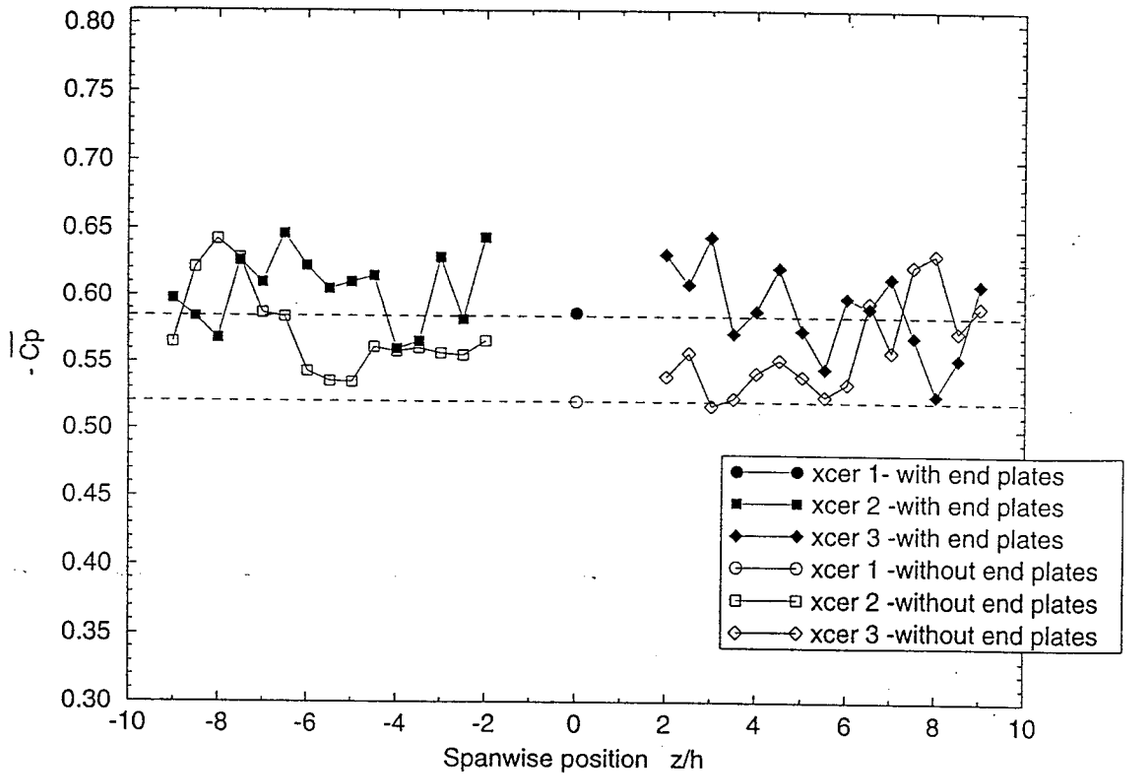

FIGURE 3: Mean Base Pressure Coefficient
-Turbulent Boundary Layer-

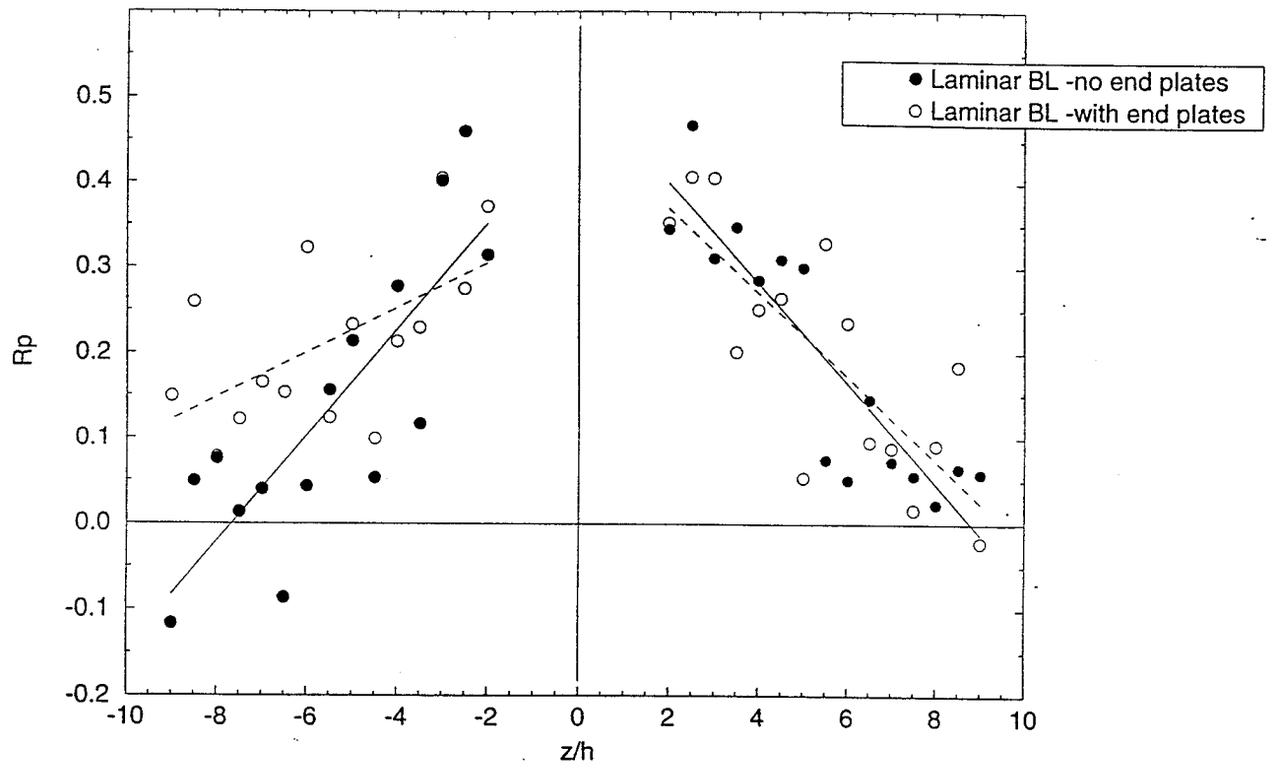

FIGURE 4: Spanwise Correlation Coefficient
-Laminar Boundary Layer-

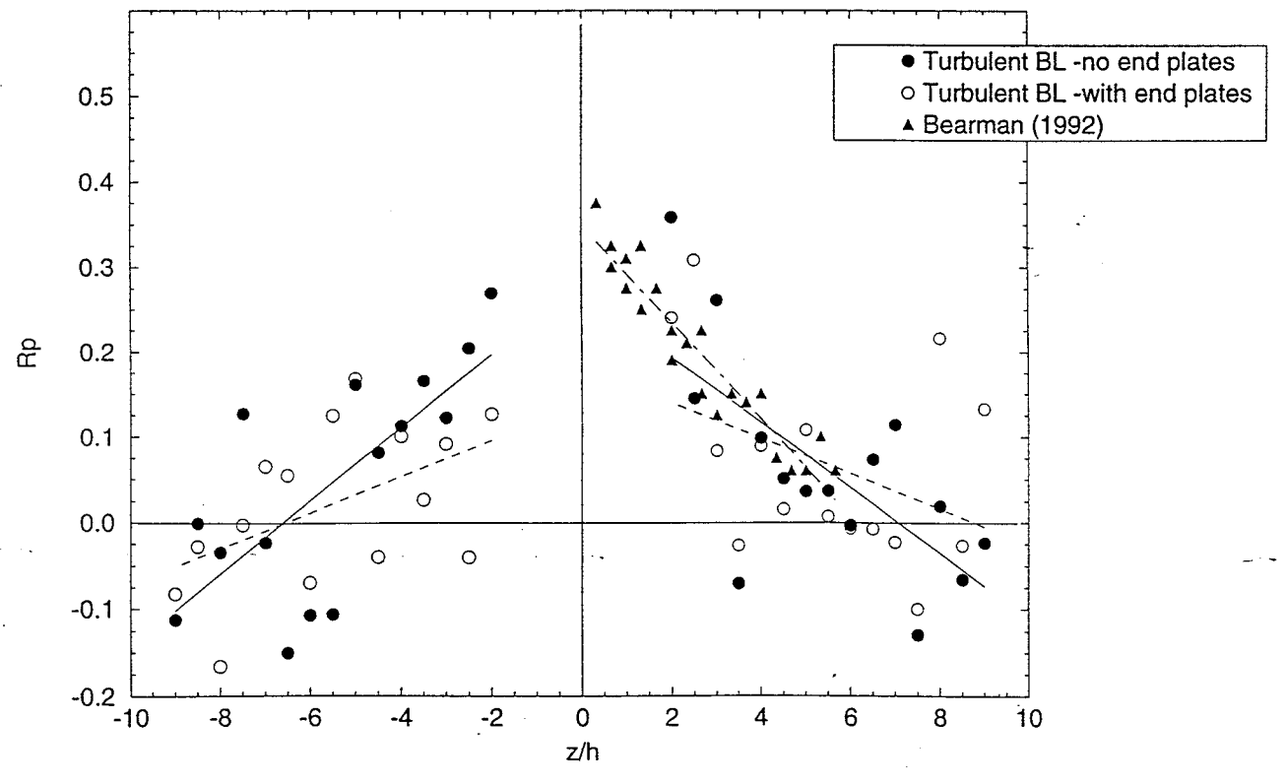

FIGURE 5: Spanwise Correlation Coefficient
-Turbulent Boundary Layer-

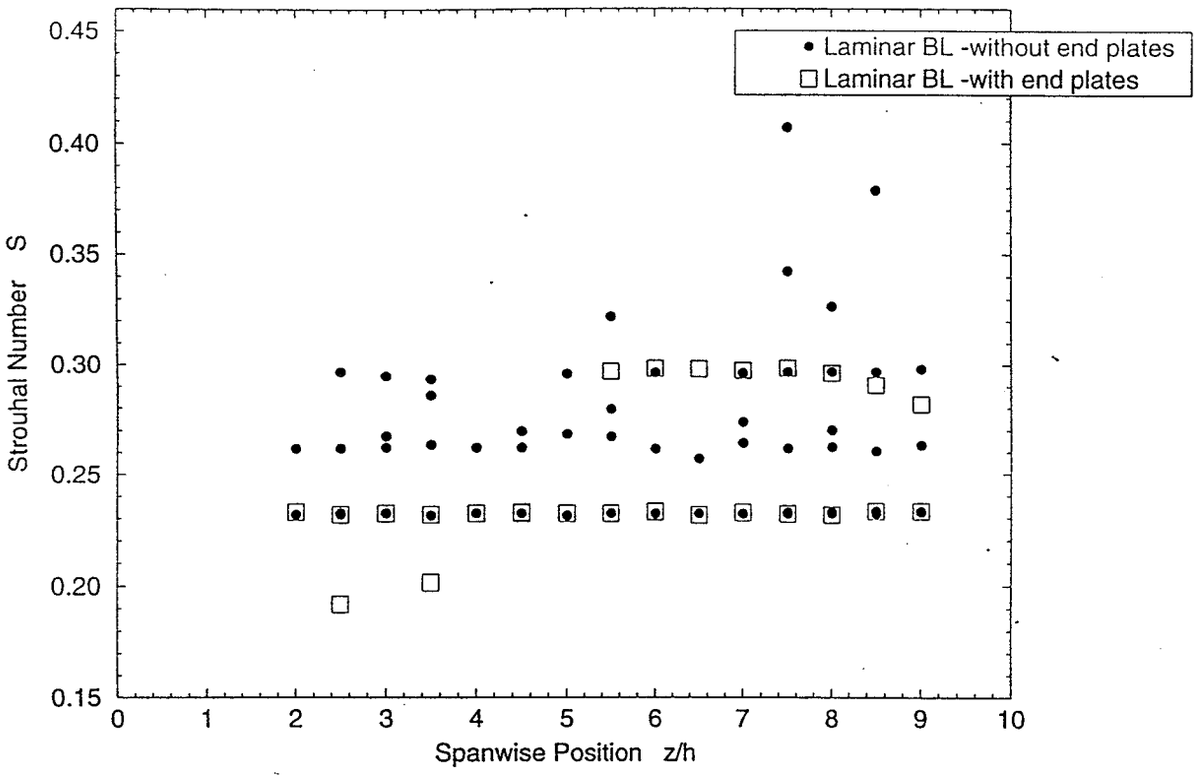

FIGURE 6: Strouhal Number vs Spanwise Position
-Laminar Boundary Layer-

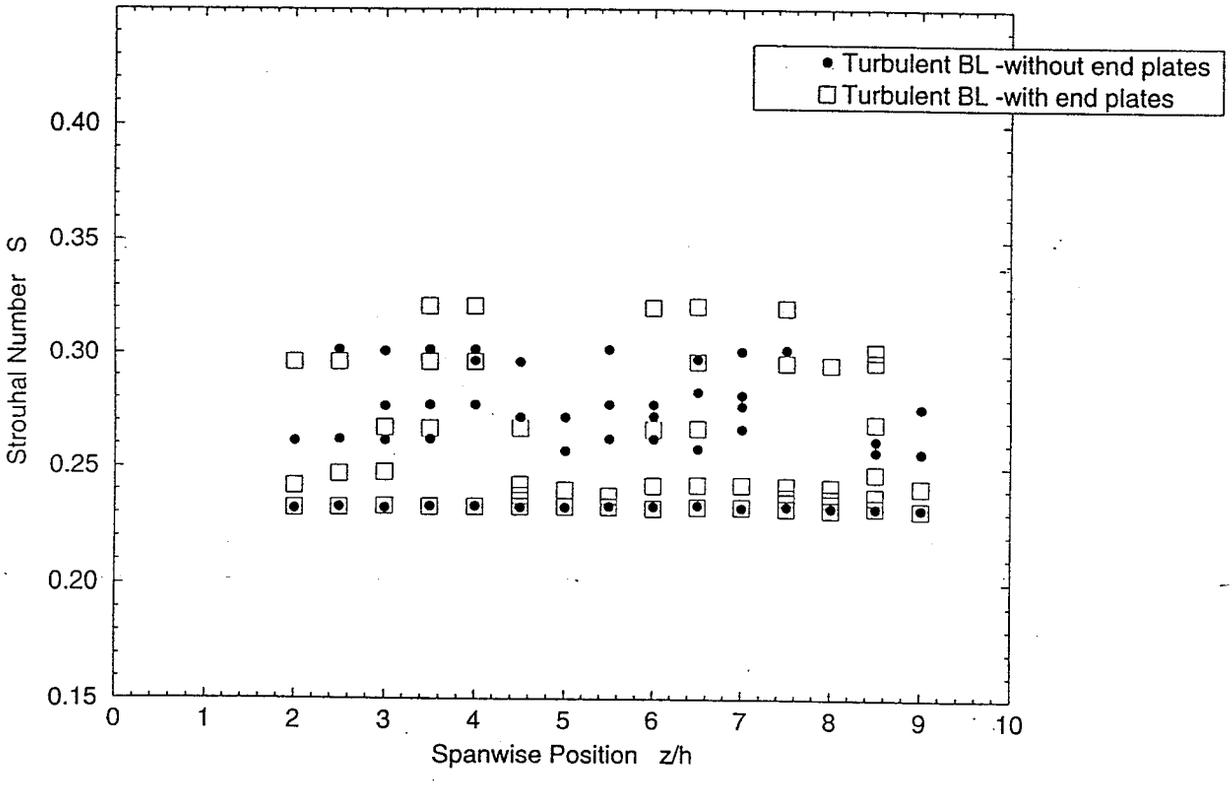

FIGURE 7: Strouhal Number vs Spanwise Position
-Turbulent Boundary Layer-